

A study of rotor eccentricities effects on brushless doubly fed machines performance

Abdi Jalebi, S., Abdi, E. & McMahon, R.

Author post-print (accepted) deposited by Coventry University's Repository

Original citation & hyperlink:

Abdi Jalebi, S, Abdi, E & McMahon, R 2016, A study of rotor eccentricities effects on brushless doubly fed machines performance. in 2015 IEEE International Electric Machines & Drives Conference (IEMDC). IEEE, pp. 66-71, IEEE International Electric Machines & Drives Conference, Coeur d'Alene, United States, 10/05/15.

<https://dx.doi.org/10.1109/IEMDC.2015.7409038>

DOI 10.1109/IEMDC.2015.7409038

Publisher: IEEE

© 2016 IEEE. Personal use of this material is permitted. Permission from IEEE must be obtained for all other uses, in any current or future media, including reprinting/republishing this material for advertising or promotional purposes, creating new collective works, for resale or redistribution to servers or lists, or reuse of any copyrighted component of this work in other works.

Copyright © and Moral Rights are retained by the author(s) and/ or other copyright owners. A copy can be downloaded for personal non-commercial research or study, without prior permission or charge. This item cannot be reproduced or quoted extensively from without first obtaining permission in writing from the copyright holder(s). The content must not be changed in any way or sold commercially in any format or medium without the formal permission of the copyright holders.

This document is the author's post-print version, incorporating any revisions agreed during the peer-review process. Some differences between the published version and this version may remain and you are advised to consult the published version if you wish to cite from it.

A Study of Rotor Eccentricities Effects on Brushless Doubly Fed Machines Performance

S. Abdi, E. Abdi, *Senior Member, IEEE*, and R.A. McMahon

Abstract-- This paper studies the unbalanced magnetic pull (UMP) in the Brushless Doubly-Fed Machine (BDFM). Analytical study is performed to derive the UMP, then, Finite element (FE) analysis, which has been verified experimentally, is used to verify the analytical method. The BDFM with different types of rotor eccentricities including static and dynamic eccentricities, are also modeled in FE method and their resultant UMPs are obtained. The results are compared with the case at which a perfectly constructed rotor is considered. The study has been carried out on a prototype D400 250 kW BDFM.

Index Terms-- Brushless doubly fed machine (BDFM), finite element (FE) analysis, unbalanced magnetic pull (UMP), rotor eccentricity, parallel winding.

I. INTRODUCTION

THE brushless doubly fed machine (BDFM) is of interest as a variable speed generator or drive because only a fraction of the output power needs to pass through the power converter. The absence of brush-gear and slip-rings makes the machine particularly attractive as a wind turbine generator because brush-gear and slip-ring problems in the widely used doubly fed induction generator (DFIG) have been identified as a principal failure mode [1]. Studies indicate that the combination of a BDFM and a two-stage gearbox in a wind turbine would have excellent reliability and retain low cost [2].

The authors have successfully demonstrated a small-scale BDFM in a working 20 kW wind turbine [3] and have built a 250 kW prototype in a frame size D400 involving construction and winding techniques appropriate to large machines that has undergone witnessed tests over its full load and speed range. Other groups also have reported large BDFMs, for example in Brazil with a 75 kW machine [4]

and China with the design of a 200 kW machine [5].

The BDFM is originally a single-frame self-cascaded induction machine, in which two stator windings of different pole numbers share the same iron circuit with a rotor winding of related pole number [6]. The contemporary BDFM has two stator windings connected to different frequency supplies, producing different pole number magneto-motive forces (MMF) with no direct coupling between them, coupling being through the rotor only. The separate stator windings facilitate double feeding, with one winding connected to the grid called the power winding (PW) and the other via a partially rated power electronic converter called the control winding (CW), as shown in Fig. 1, without any winding utilisation penalty. The rotor winding carries an MMF induced by the stator windings and the rotor and stator windings are coupled by the flux rotating in the common iron circuit.

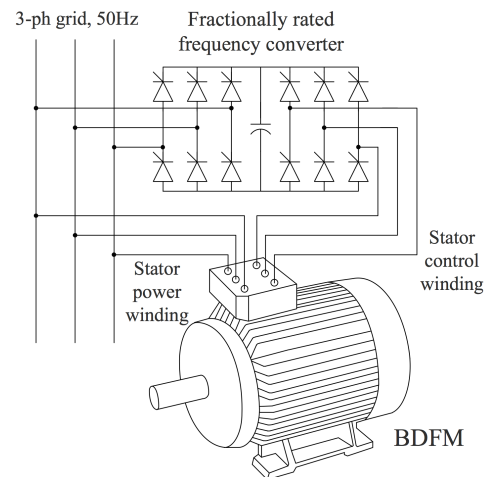


Fig. 1. Schematic of BDFM grid connection.

As with all induction type machines, characterized by relatively small air gaps, the strong magnetic fields across the air gap exert considerable forces on the iron parts of the machine. These cause time-varying deflections on the machine surface which lead to vibration and acoustic noise. One source of producing deflection is unbalanced magnetic pull (UMP), which can be mathematically shown as the interaction between two air gap flux waves with pole-pair

The research leading to these results has received funding from the European Union's Seventh Framework Program managed by REA Research Executive Agency (FP7/2007 2013) under Grant Agreement N.315485.

S. Abdi, and R.A. McMahon are with the Electrical Engineering Division, Cambridge University, Cambridge, CB3 0FA (e-mail: s.abdi.jalebi@gmail.com, ram1@eng.cam.ac.uk).

E. Abdi is with Wind Technologies Limited, St. Johns Innovation Park, Cambridge, CB4 0WS, U.K. (e-mail: ehsan.abdi@windtechnologies.com)

numbers differing by one [7].

Unlike the induction motor, which has a magnetic field dominated by a single pole number component, the BDFM has principle field components at two different pole numbers and the interaction of these two components leads to more complex deflection patterns than those occur in the induction machine [8].



Fig. 2. 250 kW D400 BDFM (right front) on test bed.

The presence of rotor eccentricity in practical machines further modulates the field patterns, exacerbating the resulting vibration. An eccentric rotor motion occurs when the rotor axis is not aligned with the axis of the stator bore. Due to manufacturing tolerances, wear of bearings, and other reasons, some degree of rotor eccentricity is always present. Rotor whirling generates an electromagnetic force also known as UMP that acts between the rotor and stator. This force can be resolved into two components: the radial force, acting in the direction of the shortest air gap; and the tangential force, which is perpendicular to the radial force. The amplitude and direction of the latter force depend on the operating condition of the machine, whirling frequency and rotor radius. Acting roughly in the direction of the shortest air gap, UMP tends to further increase the eccentricity magnitude and may cause serious damage to the machine or even the whole drive. In addition, UMP acts as a major source of vibration and acoustic noise.

A detailed study of UMP and its resultant displacement in stator back iron for the BDFM is presented in this paper taking the effects of rotor eccentricity into account. Analytical methods are commonly used to study the electromagnetic forces due to rotor eccentricity, for example in [9-11], however such methods are not sufficient when accurate assessment of rotor eccentricity, iron saturation effects, and stator and rotor slotting is required. In addition, the complex magnetic field pattern in the BDFM air gap resulting from the two stator fields with different pole numbers and frequencies makes an analytical study difficult.

A 2-D time-stepping Finite Element (FE) modeling which has been verified experimentally for a D400 250 kW

prototype BDFM is therefore utilized. FE analysis has been widely used, for example in [12-16], to study UMP and its resulting vibration in electrical machines. The drawback of FE modeling is that in the presence of eccentricity, there is no geometric symmetry, so the whole cross section of the machine must be modeled. This results in an FE mesh with a large number of elements as reported by others such as [17], [18] making the analysis time consuming.

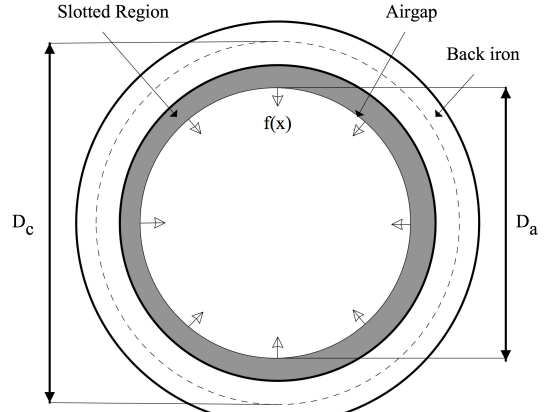


Fig. 3. BDFM Stator subjected to magnetic pull

II. PROTOTYPE MACHINE CONSIDERED IN THIS STUDY

The specifications of the 250 kW BDFM are shown in Table I. The D400 BDFM was constructed as a frame size D400 machine with the stack length of 820 mm. The stator windings were form wound from copper strips. The power winding was rated at 690 V, 178 A, at 50 Hz and the control winding was designed for 620 V at 18 Hz and rated at 73 A. Both stator windings were connected in delta. The rotor comprises six sets of nests each consisting of a number of concentric loops [19], the conductors being solid bars with one common end ring [20]. The magnetic properties for the iron were provided by the machine manufacturer. The D400 BDFM on test bed is shown in Fig. 2.

TABLE I
Specifications of the 250kW D400 BDFM

Frame size	400
PW pole number	4
PW rated voltage	690V at 50 Hz (delta)
PW rated current	178 A (line)
CW pole number	8
CW rated voltage	620 V at 18 Hz (delta)
CW rated current	73 A (line)
Speed range	500 rpm \pm 36%
Rated torque	3670 Nm
Rated power	250 kW at 680 rpm
Efficiency (at full load)	> 95%
Stack length	0.82 m

III. MAGNETIC FORCES AND RESULTING DEFLECTION

The radial forces exerted by the air gap magnetic field on the stator tooth tops are calculated. The effect of tangential forces on the teeth which ultimately exert torque to the machine's shaft are not considered in this analysis [9]. Fig. 3 shows the schematic of the BDFM stator. The air gap magnetic field is essentially the superposition of two field components, one with $2p_1$ poles, the mean absolute flux density of \bar{B}_1 rotating at ω_1 rad/s and another with $2p_2$ poles, \bar{B}_2 flux density rotating at ω_2 . The total flux density as a function of space angle and time is therefore:

$$B(\theta, t) = \frac{\pi}{2} [B_1 \cos(p_1 + \omega_1 t + \phi_1) + B_2 \cos(p_2 + \omega_2 t + \phi_2)] \quad (1)$$

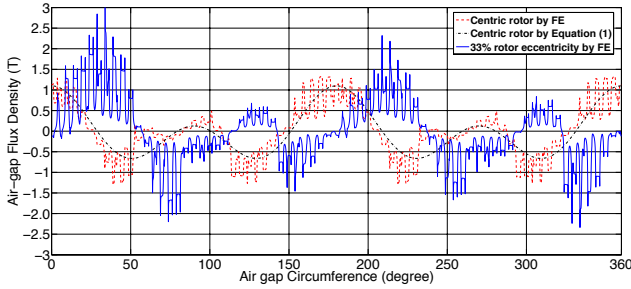


Fig. 4. Air gap flux density obtained from (1) and FE modeling when the rotor is centric and eccentric. Results are obtained from frozen fields at different times, so the relative phase shift is arbitrary.

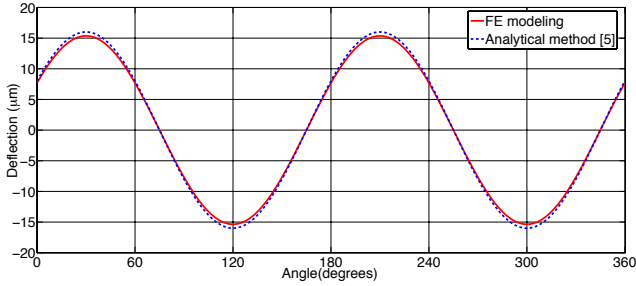


Fig. 5. Comparison of displacements in the stator back iron when the rotor is centric obtained from FE modeling and analytical method

where ω_1 and ω_2 are the frequencies of the two stator supplies, and, ϕ_1 and ϕ_2 are phase offsets. Any harmonic field components created by the rotor structure, slotting, saturation and rotor eccentricity are ignored in (1). In Fig. 4, a typical air gap field for a 4/ 8 pole BDFM at the point where t and ϕ terms are zero is shown in black, i.e. the smooth line. The field represents magnetic loading of 0.48 T, which is the design value for the 250 kW BDFM. The air gap flux density obtained from 2-D linear FE modeling which takes into account all the harmonic components mentioned above is also shown in Fig. 4 for a centric rotor. The magnetic field in the air gap exerts an inward force on the stator tooth top and an equal and opposite outwards force on the rotor tooth tops. At any point the force is

related to the magnetic field strength by [21]

$$f = \frac{B^2(\theta, t)}{2\mu_0} \quad (2)$$

This force will cause the stator back iron to deflect, which is estimated using 1-dimensional beam theory as proposed by Alger [22]. The force must be balanced by elastic deformation of the back iron and the frame. The force in the air gap may be replaced by an equivalent force at the central axis of the back iron (the dashed line in Fig. 3) given as a function of the mechanical angle by

$$f_b(\theta, t) = \frac{D_a B^2(\theta, t)}{D_c 2\mu_0} \quad (3)$$

where D_a is the air gap diameter and D_c is the diameter at the center of the back iron. The force can be considered as the superposition of two components, the average force which causes a small deflection constant in θ and can be neglected [8], and the space varying component given by

$$f'_b(\theta, t) = f_b(\theta, t) - \frac{1}{2\pi} \int_0^{2\pi} f_b(\theta, t) \cdot d\theta \quad (4)$$

Next, the deflection resulted from this applied force can be calculated. The force is resisted mainly by the stator back iron, as the machine's frame makes negligible contribution to resisting the magnetic forces due to its much lower bending stiffness [8]. The shear stress S in the beam is related to the force by

$$S(\theta, t) = \frac{D_c l}{2} \int f'_b(\theta, t) \cdot d\theta \quad (5)$$

The shear stress is the differential of the bending moment, M and therefore

$$M(\theta, t) = \frac{D_c}{2} \int S(\theta, t) \cdot d\theta \quad (6)$$

Finally the deflection, $v(\theta, t)$ due to the loading is given by the double integral of the bending moment

$$v(\theta, t) = -\frac{D_c^2}{4} \frac{12}{E_{ym} l y_c^3} \int \int M(\theta, t) \cdot d\theta \quad (7)$$

where E_{ym} is the Young's Modulus of the material, y_c is the core back depth and l is the stator stack length. In the present study, the air gap flux density, $B(\theta, t)$, is obtained from FE modeling. Then from (2) to (7), the stator back iron displacement is obtained. Fig. 5 shows the deflection obtained from the method described above and from the experimentally verified analytical method given in [8]. As can be seen, there is close agreement between the two results, validating the approach used in this paper to calculate deflection.

IV. EFFECTS OF ROTOR ECCENTRICITIES

The radial forces acting on the surface of the rotor are

very large but cancel each other when the rotor axis is aligned with the stator axis. Similarly, tangential forces are balanced such that only an axially rotating moment is produced. If the rotor is eccentric, then UMP occurs. The phenomenon can be described as an imbalance of the radial and tangential forces acting on the rotor (or stator) surface such that a net radial force is developed. This can result in vibration and noise, and increase the possibility of the stator and rotor contact.

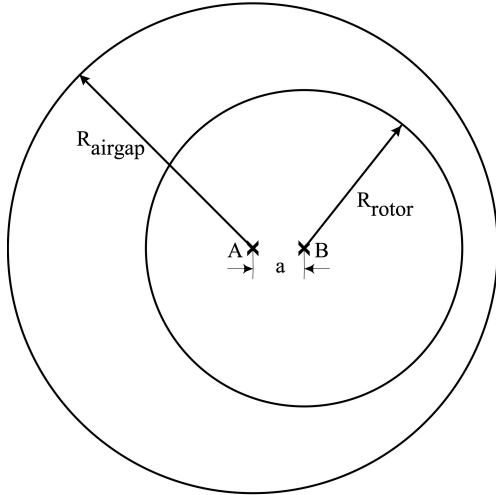


Fig. 6: Static eccentricity when the rotor center (B) is not aligned with the stator center (A). The position of B is constant with time and the level of eccentricity is 'a'.

The UMP due to eccentricity takes two forms: static and dynamic. Static UMP is caused by the rotor axis being positioned parallel to, rather than being on, the stator axis as a result of manufacturing tolerances. In this case, the rotor is rotating around its own axis, see Fig. 6. Dynamic UMP occurs when the rotor is precessing about the stator bore center but not its own center, see Fig. 7. This could be produced by manufacturing tolerances or rotor whirl near a critical speed. Different levels of static and dynamic eccentricities when the rotor is off-center by 33%, 21%, and 7% of the nominal air gap length are considered in this study. The level of eccentricity referred to in the following text is always expressed as percentage of the nominal air gap length.

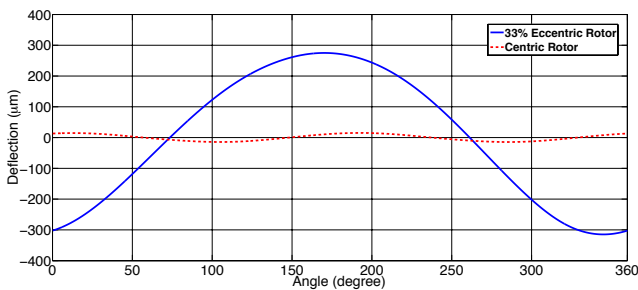


Fig. 8. Displacement in the stator back iron when the rotor is centric and when the rotor is 33% eccentric.

The air-gap magnetic flux density distribution frozen in time for a perfectly constructed BDFM with uniform air gap and specifications given in Table I, and the case when the rotor is statically eccentric by 33%, are shown in Fig. 4. It is obvious from the figure that some regions of the non-uniform air gap experience high level of flux density, up to 3 T. As shown in Fig. 8, this high flux density level results in a deflection which is significantly i.e. 18 times larger than the case of an ideally constructed machine. Therefore, the mitigation of UMP is important in the BDFM if standard manufacturing tolerances are allowed.

Parallel connection of stator coils is widely used to reduce UMP in electrical machines with non-uniform air gaps and its effects have been discussed in the literature, for example in [23]. Effectively, the variation of reluctance due to uneven air gap length causes circulating currents in the parallel paths, which improve the air gap flux distribution, hence reducing the deflection and UMP.

Connecting the stator coils in parallel in a BDFM is not as straightforward as in other electrical machines. The main reason is that parallel connection of stator coils may lead direct coupling of stator windings if not considered carefully. The large circulating currents produced by direct coupling will cause significant losses and degrade machine performance.

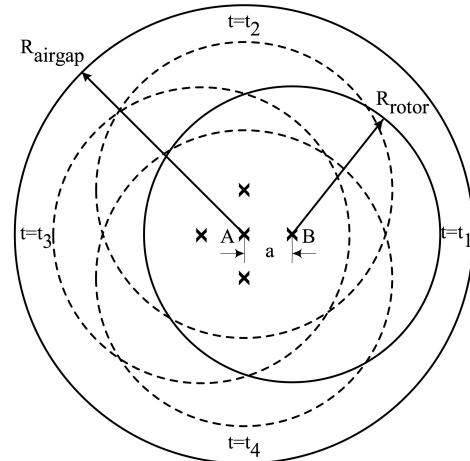


Fig. 7: Dynamic eccentricity when the rotor center (B) is not aligned with the stator center (A). The position of B varies with time, but the level of eccentricity 'a' remains constant.

V. RESULTS AND DISCUSSION

The 250 kW BDFM when operating in the synchronous mode is modeled in FE using a time stepping method. The FE models are verified by experimental results reported in [23]. The PW and CW are supplied at 50 Hz and 15 Hz respectively at their rated voltages. Fig. 9 shows the magnetic flux in the cross section of the machine. Centric rotor as well as different static and dynamic eccentric rotors described in section IV are studied. For each model, the

space distribution of air gap flux density is extracted. Using the air gap flux density and (2) to (7), the stator back iron deflection is derived.

Table II

The *rms* value of displacement obtained from FE modeling for static and dynamic eccentricities

Eccentricity	Displacement (μm)		
	7%	21%	33%
Static	43	125	214
Increase	3.5 times	10.5 times	18 times
Dynamic	29	67	137
Increase	2.5 times	5 times	11.5 times

Different levels and types of rotor eccentricity are studied in this paper. The back iron displacement for static (Fig. 6) and dynamic (Fig. 7) eccentricities are shown in Figs. 10 and 11, respectively. The *rms* values of displacement for the above cases are also calculated and shown in Table II. As it is clear significant increase (up to 18 times in static eccentricity) can be observed compare to when the rotor is ideally constructed. In addition, the amount of increase in static eccentricity is higher in all different levels compare to when the dynamic eccentricity is existed.

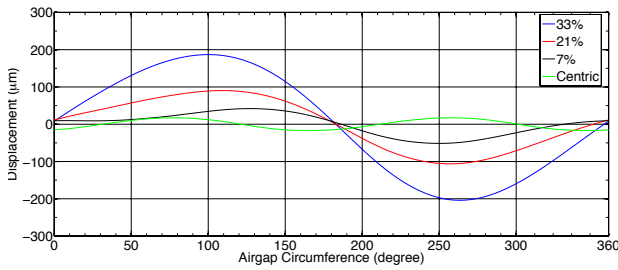


Fig. 10. Stator back iron deflection for different levels of rotor static eccentricities shown in Fig. 6

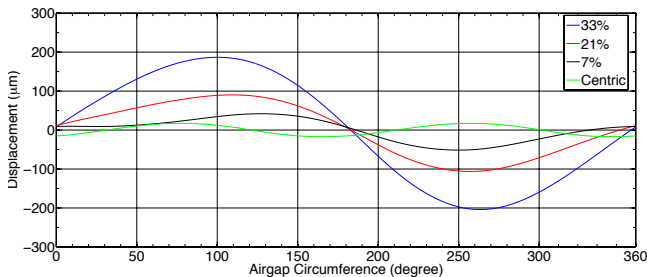


Fig. 11. Stator back iron deflection for different levels of rotor dynamic eccentricities shown in Fig. 7

VI. CONCLUSION

This paper has provided the analysis of the UMP caused by the fundamental fields in the BDFM which allows its magnitude to be calculated and compared with those in conventional machines. The theoretical predictions have been validated numerically using FE modeling and

analysis. The presence of two components of the magnetic field in the air gap with different pole numbers give rise to the UMP magnitude that do not occur in single field machines like the induction motors. This high amount of UMP can be a key source of vibration and noises in the BDFM.

The rotor eccentricity, caused by manufacturing tolerances, wear of bearings, and other reasons, further modulates the field patterns and exacerbating the resulting vibration. Rotor whirling generates an electromagnetic force and hence UMP that acts between the rotor and stator, resulting in much more vibration and noise, and increase the possibility of the stator and rotor contact. Different types of rotor eccentricities including static and dynamic eccentricity have been studied in this paper and their effects are considered in terms of the stator back iron displacement. The displacement is showing to be scaled up by several times in different levels of rotor eccentricity, compare to where the centric rotor is modeled.

Consequently, actions must be taken in order to mitigate the UMP and its resulting vibration in a BDFM to acceptable levels. More accurate design and manufacturing process for the BDFM rotor and its bearings to reduce the air gap non-uniformity is required. Furthermore, reinforcing the stator back iron stiffness by increasing the back iron thickness, and paralleling the stator winding coils can be employed in order to have a BDFM with less vibration and noise levels.

VII. REFERENCES

- [1] H. Arabian-Hoseynabadi, H. Oraee, and P. J. Tavner, "Wind turbine productivity considering electrical subassembly reliability," *Renewable Energy*, no. 35, pp. 190–197, 2010.
- [2] P. Tavner, A. Higgins, H. Arabian, H. Long, and Y. Feng, "Using an FMEA method to compare prospective wind turbine design reliabilities," *Poland: Proc. European Wind Energy Conf. (EWEC 2010)*, 2010, pp. 1–10.
- [3] T. Logan, J. Warrington, S. Shao, and R. A. McMahon, "Practical deployment of the brushless doubly-fed machine in a medium scale wind turbine," *Taiwan: Eighth International Conference on Power Electronics and Drive Systems*, November 2009.
- [4] R. Carlson, H. Voltolini, F. Runcos, P. Kuo-Peng, and N. Baristela, "Performance analysis with power factor compensation of a 75 kw brushless doubly fed induction generator prototype," *IEEE International Conference on Electric Machines Drives*, 2010.
- [5] H. Liu and L. Xu, "Design and performance analysis of a doubly excited brushless machine for wind power generator application," *IEEE International Symposium on Power Electronics for Distributed Generation Systems*, 2010, pp. 597 – 601.
- [6] P. C. Roberts, R. A. McMahon, P. J. Tavner, J. M. Maciejowski, and T. J. Flack, "Equivalent circuit for the brushless doubly fed machine (bdfm) including parameter estimation and experimental verification," *Electrical Power Applications, IEE Proceedings*, vol. 152, no. 4, pp. 933–942, July 2005.
- [7] D. Dorrell, A. knight, and R. Betz, "Issues with the design of brushless doubly-fed reluctance machines: unbalanced magnetic pull, skew and iron losses," *IEEE Int. Electric Machines and Drives Conf (IEMDC)*, 2011, pp. 663 – 668.
- [8] T. Logan, R. McMahon, and K. Sffen, "Noise and vibration in brushless doubly fed machine and brushless doubly fed reluctance machine," *IET Electric Power Applications*, vol. 7, pp. 1 – 10, 2014.

- [9] D. Dorrell and A. Smith, "Calculation of u.m.p in induction motors with series or parallel winding connections," *IEEE Transactions on Energy Conversion*, vol. 9, pp. 304 – 310, 1994.
- [10] A. Stavrou and J. Penman, "Modeling dynamic eccentricity in smooth air-gap induction machines," *IEEE Int. Electric Machines and Drives Conf (IEMDC)*, 2001, pp. 864 – 871.
- [11] R. Robinson, "The calculation of unbalanced magnetic pull in synchronous and induction motors," *AIEE Trans*, vol. 62, pp. 620 – 624, 1943.
- [12] A. Burakov and A. Arkkio, "Comparison of the unbalanced magnetic pull mitigation by the parallel paths in the stator and rotor windings," *IEEE Transactions on Magnetics*, vol. 43, pp. 4083 – 4088, 2007.
- [13] M. DeBortoli, S. Salon, and C. Slavik, "Effects of rotor eccentricity and parallel windings on induction machine behaviour: A study using finite element analysis," *IEEE Transactions on Magnetics*, vol. 29, pp. 1676-1682, 1993.
- [14] D. Zarko, D. Ban, I. Vazdar, and V. Jaric, "Calculation of unbalanced magnetic pull in a salient pole synchronous generator using finite element method and measured shaft orbit," *IEEE Transactions on Industrial Electronics*, vol. 59, pp. 2536 – 2548, 2012.
- [15] D. Dorrell and D. Ionel, "Radial forces and vibrations in permanent magnet and induction machines," *IEEE Power and Energy Society General Meeting*, 2012, pp. 1 – 6.
- [16] M. Berman, "On the reduction of magnetic pull in induction motors with off-centre rotor," *IEEE Industrial Application Society Annual Meeting*, 1993, pp. 343 – 350.
- [17] R. Perers, U. Lundin, and M. Leijon, "Saturation effects on unbalanced magnetic pull in a hydroelectric generator with an eccentric rotor," *IEEE Transactions on Magnetics*, vol. 43, no. 10, pp. 3884 – 3890, 2007.
- [18] L. Wang, R. Cheung, Z. Ma, J. Ruan, and Y. Peng, "Finite element analysis of unbalanced magnetic pull in a large hydro generator under practical operations," *IEEE Transactions on Magnetics*, vol. 44, no. 6, pp. 1558 – 1561, 2009.
- [19] R. McMahon, P. Tavner, E. Abdi, P. Malliband, and D. Barker, "Characterising brushless doubly fed machine rotors," *IET Electric Power Applications*, vol. 7, pp. 535 – 543, 2013.
- [20] R. A. McMahon, E. Abdi, P. Malliband, S. Shao, M. E. Mathekgwa, and P. J. Tavner, "Design and testing of a 250 kw brushless dfig," Bristol, UK: 6th IET International Conference on Power Electronics, Machines and Drives (PEMD), March 2012.
- [21] B. Heller and V. Hamata, *Harmonic Field Effects in Induction Machines*. Elsevier Scientific Publishing Company, 1977.
- [22] P. Alger, *The Nature of Polyphase Induction Machines*. New York: John Wiley and Sons, 1951.
- [23] R. Hellmund, "Series versus parallel windings for a.c machines," *Electrical World*, 49:388-389, 1907.
- power electronics and semiconductor materials.

VIII. BIOGRAPHIES

Salman Abdi received his BSc degree from Ferdowsi University, Mashhad, Iran, in 2009 and M.S.c degree from Sharif University of Technology in 2011, both in electrical engineering. He is currently working toward the PhD degree at Cambridge University in electrical machines design and modelling. His main research interests include electrical machines and drives for renewable power generation.

Ehsan Abdi (SM' 2012) received his BSc degree from Sharif University of Technology in 2002 and his MPhil and PhD degrees from Cambridge University in 2003 and 2006 respectively, all in Electrical Engineering. Currently, he is the Managing Director of Wind Technologies Ltd where he has been involved with commercial exploitation of the brushless doubly fed induction generator technology for wind power applications. His main research interests include electrical machines and drives, renewable power generation, and electrical measurements and instrumentation.

Richard McMahon received the degrees of BA (in Electrical Sciences) and PhD from Cambridge University in electrical engineering, in 1976 and 1980 respectively. Following postdoctoral work on semiconductor device processing he was appointed University Lecturer in Electrical Engineering at Cambridge University Engineering department in 1989 and became a Senior Lecturer in 2000. His research interests include electrical drives,